Low altitude unmanned aerial vehicle for characterising remediation effectiveness following the FDNPP accident

Martin, P.G.; Payton, O.D.; Fardoulis, J.S.; Richards, D.A.; Yamashiki, Y.; Scott, T.B.

Journal of Environmental Radioactivity 151 (2016) 58–63

Contents lists available at ScienceDirect

Journal of Environmental Radioactivity

journal homepage: www.elsevier.com/locate/jenvrad

Low altitude unmanned aerial vehicle for characterising remediation effectiveness following the FDNPP accident

P.G. Martin [a, *], O.D. Payton [a], J.S. Fardoulis [a], D.A. Richards [b], Y. Yamashiki [c], T.B. Scott [a]

[a] Interface Analysis Centre, HH Wills Physics Laboratory, University of Bristol, Bristol, BS8 1TL, UK
[b] Bristol Isotope Group, School of Geography, University Walk, Bristol, BS8 1SS, UK
[c] Graduate School of Advanced Integrated Studies in Human Survivability, Kyoto University, Kyoto, 606-8501, Japan

ARTICLE INFO

Article history:
Received 17 May 2015
Received in revised form
25 August 2015
Accepted 6 September 2015
Available online 26 September 2015

Keywords:
Fukushima
UAV
Gamma-spectrometry
Decontamination
Remediation

ABSTRACT

On the 12th of March 2011, The Great Tōhoku Earthquake occurred 70 km off the eastern coast of Japan, generating a large 14 m high tsunami. The ensuing catalogue of events over the succeeding 12 d resulted in the release of considerable quantities of radioactive material into the environment. Important to the large-scale remediation of the affected areas is the accurate and high spatial resolution characterisation of contamination, including the verification of decontaminated areas. To enable this, a low altitude unmanned aerial vehicle equipped with a lightweight gamma-spectrometer and height normalisation system was used to produce sub-meter resolution maps of contamination. This system provided a valuable method to examine both contaminated and remediated areas rapidly, whilst greatly reducing the dose received by the operator, typically in localities formerly inaccessible to ground-based survey methods. The characterisation of three sites within Fukushima Prefecture is presented; one remediated (and a site of much previous attention), one un-remediated and a third having been subjected to an alternative method to reduce emitted radiation dose.

1. Introduction

Following the accident at the Fukushima Daiichi Nuclear Power Plant (FDNPP) initial measurements of radiation intensity, dose and distribution were performed using manned military and civilian aircraft at high altitudes of 150–700 m to provide early quantifications across the east of Japan (MEXT, 2011; Sanada et al., 2014b). Utilising these survey methods it was possible to quickly understand the approximate distribution of radio-caesium contamination across a very large area, independent of terrain. However, due to Japanese aviation law, manned helicopters are prohibited from flying at altitudes lower than 150 m, preventing higher spatial resolution surveys. Working at reduced altitudes closer to the contamination source risks exposing aircrew and operators to heightened, potentially dangerous, levels of radiation. In contrast, foot-based surveys of radiological contamination following events at the Japanese plant, despite being highly detailed with an improved spatial resolution, are considerably more time and cost consuming. Additional negatives, again, come from the elevated radiation levels workers are exposed to when conducting this work as well as the inability to undertake measurements in inaccessible areas, e.g. forests, paddy fields and rooftops. In addition to exposing themselves to radiation whilst undertaking the survey; individuals can attenuate circa 30% of the incident gamma-rays - affecting the survey's results (Jones and Cunningham, 1983).

A bridge between manned high altitude aircraft surveys and foot based measurements has been established by Sanada (Sanada and Torii, 2014; Sanada et al., 2014a). An autonomous unmanned helicopter, more commonly used for automated crop dusting, weighing 94 kg with a payload of three $LaBr_3$:Ce scintillator detectors totalling 6.5 kg, conducted airborne mapping of radiation at a maximum speed of 8 m/s and altitude of 80 m above ground level. This method produced an improved ground sampling resolution of 80 m mesh per pixel, thereby offering a significant improvement over higher altitude surveys.

Much work is currently ongoing to remediate land and structures contaminated by the Fukushima incident, with recent estimates placing the likely total cost at 5 trillion yen (National Institute of Advanced Industrial Science and Technology (2014)). Central to this clean-up is the accurate determination of the location and isotopic nature of the emitted contamination prior to, as

* Corresponding author.
E-mail address: peter.martin@bristol.ac.uk (P.G. Martin).

http://dx.doi.org/10.1016/j.jenvrad.2015.09.007

well as following cleaning. A wide variety of methods have so far been employed in the clean-up operation (Hardie and McKinley, 2014), including, but not limited to; high pressure washing, grit blasting, the physical removal of surface material or the addition of clean, blanketing sand/sediment layers onto surfaces to attenuate radiation and provide shallow burial of the problem.

The use of a light weight multi-rotor unmanned aerial vehicle (UAV) is shown herein to be powerful tool in assessing contamination, both prior to, and following remediation efforts in addition to charting the environmental migration of radionuclides through natural (fluvial) processes. Such a system is capable of producing plots of radiation intensity down to the meter-scale with full isotopic fingerprinting.

2. Materials and methods

2.1. Unmanned aerial vehicle

The development of the UAV and radiation detection system is detailed fully in MacFarlane et al., 2014 (MacFarlane et al., 2014) and its initial application in Martin et al., 2015 (Martin et al., 2015), with the X8 multi-rotor system used for this work being specially designed and constructed in-house at the University of Bristol (Fig. 1). The multi-rotor system was 1.3 m in diameter, with a height of 0.5 m, weighing 7.0 kg and had a maximum payload capacity of 5.0 kg. Unlike large helicopters already used in Japan for radiation monitoring which use petrol engines, lithium polymer batteries were used to power the UAV with a typical flight time of 30–35 min per full charge, depending on operational conditions.

Control of the system was co-ordinated via the open-source Arducopter (APM version 2.5) autopilot system (diydrones.com), whilst both take-off and landing were performed manually using conventional remote controls, once airborne, the UAV conducted radiation mapping autonomously using preprogrammed waypoints and altitudes. An on-board high frequency (10 Hz) GPS unit ensured high spatial precision when coupled with an on-board barometric pressure sensor. A live first-person-view (FPV) video stream was transmitted from the UAV to the operator to assist in piloting as well as monitoring progress of the flight.

2.2. Radiation detection and measurement

Measurement of radiological contamination was conducted using a lightweight gamma-ray spectrometer with a small volume (1 cm^3) uncollimated cadmium zinc telluride (CZT) coplanar-grid detector and a 4096 channel MCA (GR1, Kromek, Durham, UK). The energy range of the spectrometer was 30 keV to 3.0 MeV, with an energy resolution of <2.5% FWHM at 662 keV. Electronic noise on the detector was <10 keV FWHM (Kromek Group PLC, 2015). Measurements occurred at a frequency of 2 Hz, at each recorded location, a spectrum of the energy of incoming radiation was recorded in addition to the height above the ground surface, produced using a high accuracy (<10 mm at 30 m) single-point laser rangefinder (AR2500 Acuity™). The three converging data streams were gathered using a microcontroller (Arduino™ Mega ADK, Scarmagno, Italy) located on the instrument. Data was stored locally before being relayed to a base-station in near real time. In order to keep the sensors normal to the surface, independent of the attitude of the UAV, the gamma-spectrometer and single-point LiDAR were mounted on an active gimballed stage.

2.3. Data acquisition

Flights were carried out at a speed of ~1 m s^{-1}, with the instrument operated at a height of 1–5 m above the surfaces (trees, fields and roofs), but not less than 0.5 m to prevent collision. A consistent grid separation of 1.5 m between the flight lines was maintained during assessment flights wherever practical.

Three localities were chosen for this study – all within the Kawamata region of Fukushima Prefecture, contaminated by the north-west trending plume released from the plant from the 11th to the 13th of March 2011. Location 1 - a farmstead (37 35.2507N, 140 42.0800E) had not been remediated prior to the study, whilst location 2 – Yamakiya Junior High School 3 km to the north-west (37 36.1738N, 140 40.5791E) was in the process of being remediated at the time of study in May 2014. Location 3 – a homestead with surrounding fields close to the border with neighbouring Namie Town (37 34.8815N, 140 43.0810E) had not received any clean-up action, however a large region within the centre of the site had been covered with approximately 15 cm of coarse sand.

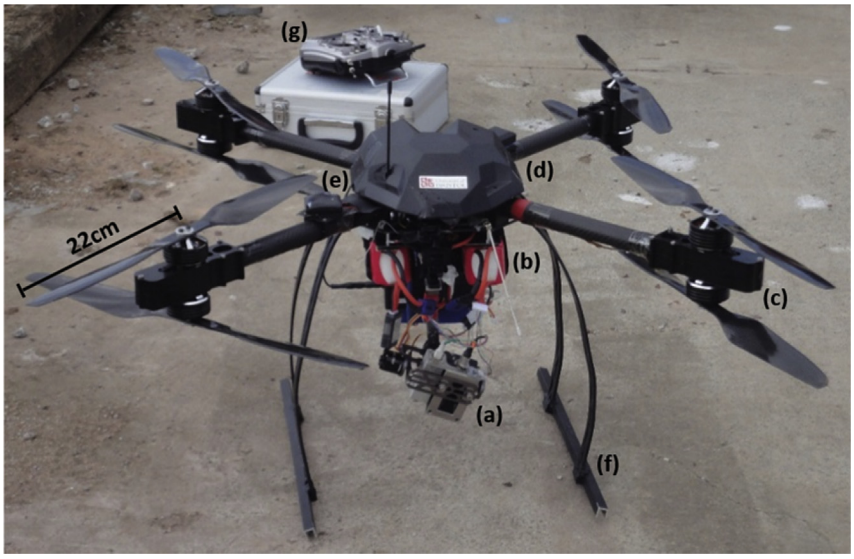

Fig. 1. Photograph of the unmanned aerial vehicle (UAV) used in the study developed at the University of Bristol: (a) detection system with detectors mounted on an active gimballed stage, (b) two lithium polymer batteries, (c) counter-rotating carbon fibre propellers, (d) domed cover over flight control system, (e) GPS unit, (f) landing gear and (g) remote control unit.

Whilst the surveys at localities 1 and 3 were performed at a constant altitude throughout, the mapping at location 2 was conducted such that the altitude of the UAV was varied to mirror the pitch of the roof - maintaining a constant 1 m separation throughout.

2.4. Data analysis

Custom analysis software was constructed to interrogate the data collected by the UAV with radiation intensity maps produced depicting radiation levels as counts per second (cps) across the entire energy range (30 keV–3.0 MeV). Each measurement point was normalised to a height of 1 m, with the possible source area of contamination on the ground existing as a function of the horizontal aperture of the detector and its altitude. A colour scaling was used to illustrate contamination levels. Each of the data points consisted of; (i) the GPS latitude and longitude location of the device, (ii) the height above the measurement surface (determined by the on-board laser rangefinder) and (iii) a gamma spectrum for the region. This gamma spectrum was converted to a cps value for the plotting of intensity. To produce the contamination map, each of the activity measurements were normalised for height above the surface using the value produced by the rangefinder following an inverse square law calculation of radiation dispersion originating from a point source (MacFarlane et al., 2014). Where ground measurement points overlapped, an average of the values detected was plotted. For previous airborne surveys collected at heights of 50–250 m (Minty, 1997; Minty et al., 1997), an exponential fall-off of radiation intensity was used to correct for detector height above the ground. Following from previous work (MacFarlane et al., 2014; Martin et al., 2015) the data arising from these surveys at lower altitudes (1–10 m) were determined to better conform to an inverse square relationship for radiation intensity with height. To establish this inverse square relationship, a series of readings were taken at numerous heights above the ground surface across the three locations in the present study as well as at a similarly contaminated site within Cornwall, England (Martin et al., 2015) using both the Kromek™ GR1 and a SAM 940 Defender Sodium Iodide detector (Berkeley Nucleonics Corporation, California, USA). After correcting these measurements to 1 m through the traditionally employed exponential decay correction and the inverse square method, it was found that the inverse square relationship produces a more accurate conversion to the value obtained at 1 m.

The calibration of the UAV mounted detection system was also performed with the SAM 940 Defender to allow for conversion of cps to dose rate. A range of sources with known activities held at differing distances were used to calibrate the system within the lab – a routine comparison within the field between the values obtained using both the GR1 and SAM 940 were performed to assure continued calibration.

3. Results and discussion

3.1. Location 1

The flight paths undertaken by the UAV at the farmstead at location 1 are shown in Fig. 2(a), with the radiation contamination maps in Fig. 2(b). A consistent moderate level of contamination, averaging 250 cps, was observed on the roof of the farmhouse building and surrounding ground surface, consistent with this site having received no formal decontamination effort prior to investigation. There appears no discernible variation across the site in measured radiation intensity, proposing little or no preconcentration within the environment or physical structure of the building, such as guttering or roof.

3.2. Location 2

As at location 1, the flight path undertaken by the UAV at locality 2: Yamakiya Junior High School is shown in Fig. 3(a), with the corresponding radiation intensity map presented in Fig. 3(b). Unlike the farm site presented in Fig. 2, this site had received considerable remediation effort as part of a study to examine possible clean-up options. Utilising the UAV over the roof of the main school building, is was possible to examine the effectiveness of this remediation.

Results from the survey (Fig. 3(b)) showed that the majority of the rooftop had low levels of contamination, averaging 35 cps, significantly below levels observed on the neighbouring ground, of

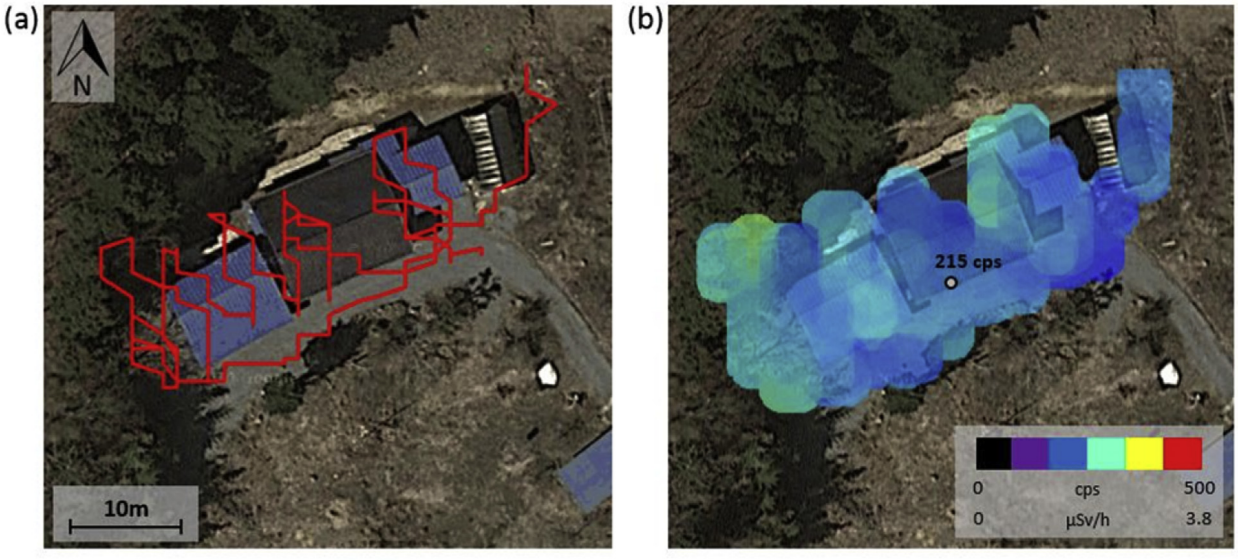

Fig. 2. (a) Flight path of the UAV over the farm buildings (Location 1) and (b) Intensity plot of detected radiation levels 1 m above the surface as counts per seconds (CPS) overlain onto the same base-map.

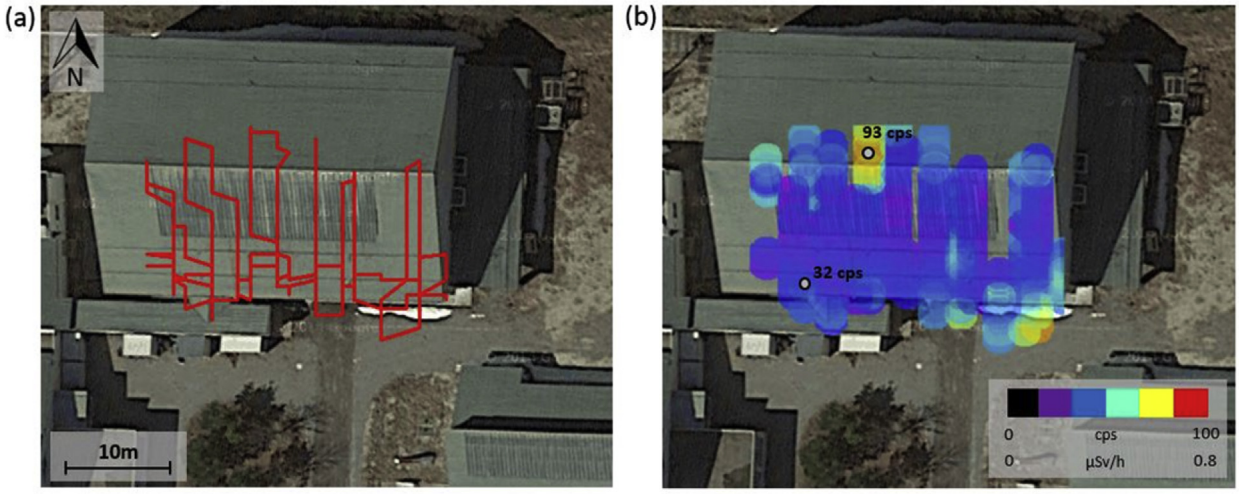

Fig. 3. (a) Flight path of the UAV over Yamakiya Junior High School (Location 2) and (b) Intensity plot of detected radiation levels 1 m above the surface as counts per seconds (CPS) overlain onto the same satellite image base-map.

60–90 cps. Apparent is the small area of elevated activity along the top, central portion of the roof, with an activity of 93 cps and dose of 0.8 µSv/h.

Despite posing little external dose risk due to the small and isolated nature of the contamination, it is shown that the unmanned aerial system is capable of locating areas of radiological interest at better than metre-scale, greatly below the 5 m mesh pixel size recently presented by Sanada et al. (Sanada and Torii, 2014). Repeated monitoring of the same areas (urban or rural) with the UAV would enable the transfer and eventual fate of this contamination in the environment to be monitored over time.

3.3. Location 3

Contrary to other methods of remediation, a vastly contrasting technique was employed at location 3: a large homestead on the border with the neighbouring Namie Town, to reduce radiation dose. Unlike at location 2, Yamakiya Junior High School (Fig. 3.) where large quantities of contaminated material were physically removed to specially designed storage sites – at this location however, a considerable volume of sand was distributed within the centre of one of its grassed fields. As is shown within Fig. 4, the central blue (in the web version) remediated portion of the map has a measurable reduction in activity when compared to the encircling outer area. The location of a quantity of material removed from the land surface with elevated radioactivity, stored within a number of 1 m^3 bags is apparent to the north-east of the site. Additional regions of higher activity exist within the surrounding forest. A detailed measure of the attenuation from the central sand covering outwards performed by the UAV is shown within Figs. 5 and 6.

The clear and rapid drop-off in activity is shown in Fig. 5(b), using the sub-meter resolution provided by the UAV. Within the

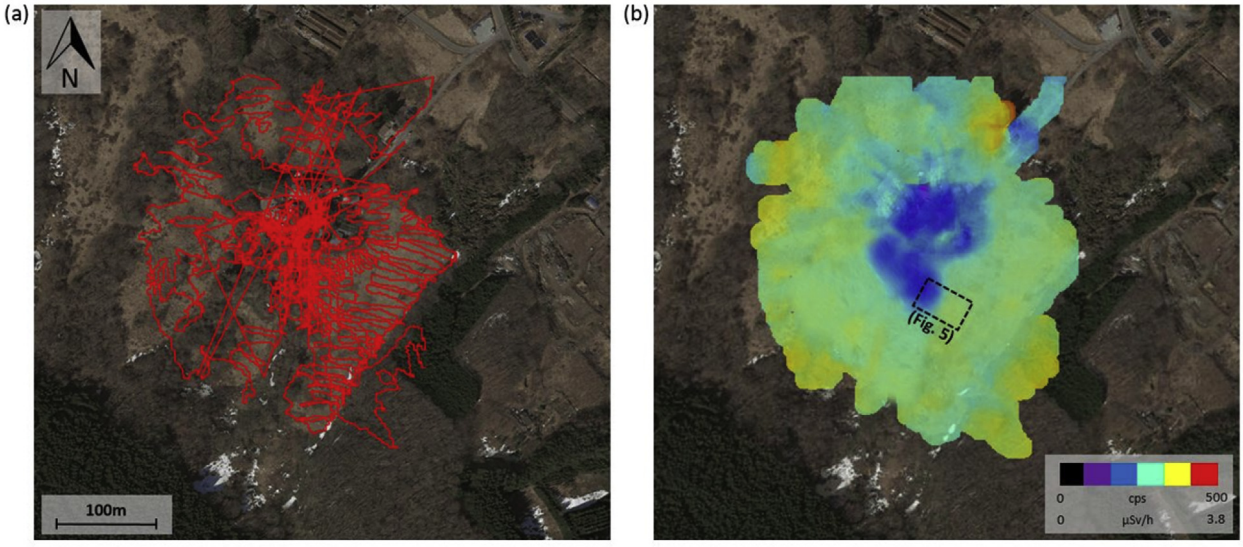

Fig. 4. Radiation contamination (CPS) map of the entire homestead calculated at 1 m above the surface (Location 3) overlain onto satellite base-map, the location of a data subset (Fig. 5.) is shown.

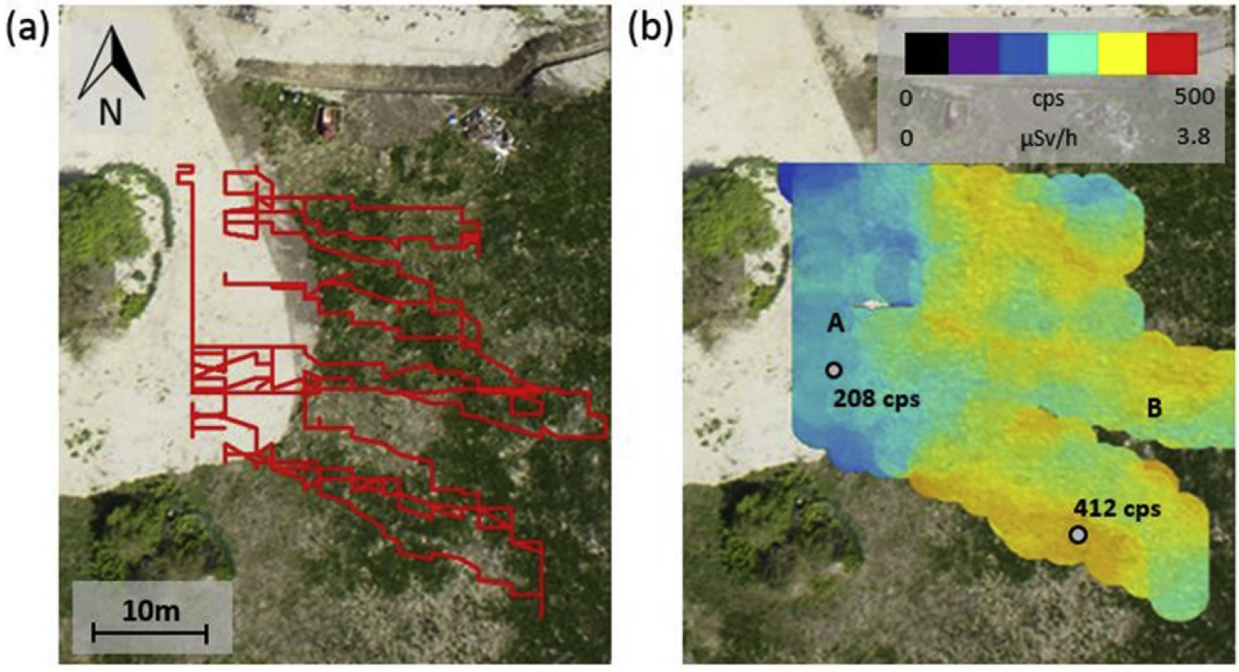

Fig. 5. (a) Flight path of the UAV over part of the homestead bordering Namie Town (location 3) as shown in Fig. 3(b) Intensity plot of detected radiation levels as counts per seconds (cps) calculated at 1 m above the surface overlain onto the same satellite image base-map.

region overlain by approximately 15 cm of coarse sand a typical activity of 208 cps was measured, however, from its coverage limit outwards a marked step is apparent. Over a distance of 10 m there was observed a two-fold increase in activity, with an average cps of 412 and dose increase from 1.8 μSv/h to 3.5 μSv/h. Such an increase is observed around the entirety of the remediated portion.

This remediation experiment presents a method in which a substantial reduction in dose is observed. However, this reduction in dose was still above long-term targeted clean-up levels of less than 1 mSv/y as part of the Act on Special Measures Concerning the Handling of Radioactive Pollution (Government of Japan (2011)) at the time of surveying and was much above levels of radionuclide activity seen at sites remediated via conventional methods such as locality 2 (Fig. 3).

3.4. Gamma spectrometry

Examining the data collected at each of the three sites enables not only the incident count rate on the CZT detector to be compared, but also the isotopic fingerprint of the contamination. The gamma spectra of the contamination from the entire flight path at each of the localities is presented in Fig. 7. Identical spectra, but with differing intensities are produced at each of the different sites, with characteristic peaks at energies corresponding to the known contaminants of ^{134}Cs and ^{137}Cs. As each of the spectra produced are identical i.e. relative intensities of the recorded gamma ray peaks remain the same, it can be assumed that the observed contamination has arisen from the same source and by association

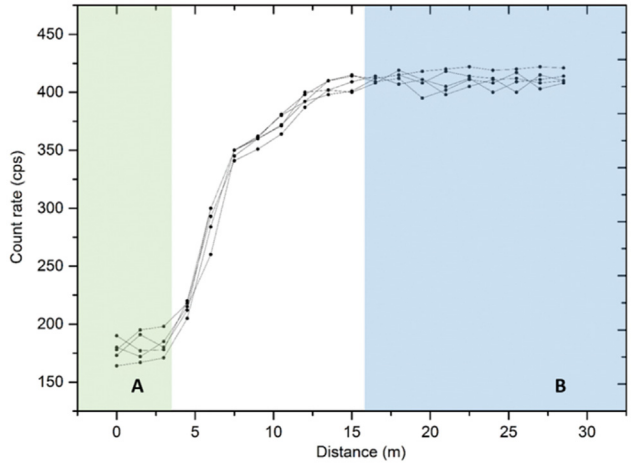

Fig. 6. Increase in activity observed from A to B (Fig. 5) from the sand covered region outwards into the surrounding field.

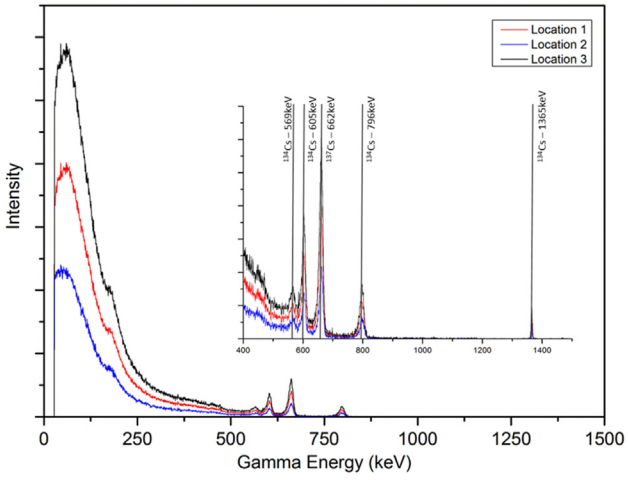

Fig. 7. Gamma energy spectrum produced from each of the three localities. Inset: characteristic energy peaks of identified isotopes.

the same dispersion event.

4. Conclusions and future work

The work presented here further demonstrates that such a small unmanned aerial system is capable of being utilised to produce radiation distribution maps at greater than 1 m resolution. Using this instrument it was able to make contamination surveys where not previously possible or practicable – such as the rooftops at locations 1 and 2. Along with radiation intensity, the instrument was also able to confirm the primary contributing radionuclides to radiation dose through analysis of the gamma-energy spectra recorded during the survey flights. Such fingerprinting is key to utilising the correct method for site remediation in addition to assessing its suitability.

Primary advantages of this unmanned aerial system over larger systems currently employed within Japan are the significantly improved spatial resolution that it can provide, its straightforward upkeep and operation, as well as its rapid deployability and ease of use at site. Greater additional advantages exist over both manned fixed-wing and helicopter systems; these include both the cost of the vehicle in addition to the dose received by those on-board. Current disadvantages of this system over larger systems include the shorter flight time, a smaller – more lightweight detector as well as a greater dependence on calm weather conditions.

Works to remediate contamination at locality 2 - Yamakiya Junior High School, are shown to be largely effective, reducing the activity levels measured at the main school building to widely accepted levels. Efforts of reducing dose at locality 3 through the addition of a blanketing layer of material to attenuate the radiation are less effective.

Future work will include extracting data collected using the single-point LiDAR unit alongside maps of radiation distribution to construct digital elevation models (DEM) of contaminated land. With such a DEM, it will be possible to combine results gained via UAV mapping with those from forensic particle studies (yielding size, shape, mass, elemental constituents etc) (Adachi et al., 2013; Mukai et al., 2014) to derive an initial particle dispersion map for the fallout which provides a baseline for subsequently modelling of radioactivity (particle) redistribution over time as a function of natural processes.

Acknowledgements

We would like to thank the University of Bristol for funding the fieldwork in association with the Institutional strategic alliance with the University of Kyoto. We would also like to thank the team at the Bristol Cabot Institute for their support and Dr Itzhak Halevy for his encouragement and inspiration for this research. We must also acknowledge Dr James MacFarlane as a valued previous member of our research team as well as the University of Bristol's Physics Workshop for their work on the air-frame. Support for fieldwork was generously provided by Sellafield Ltd and Kromek Ltd.

References

Adachi, K., Kajino, M., Zaizen, Y., Igarashi, Y., 2013. Emission of spherical cesium-bearing particles from an early stage of the Fukushima nuclear accident. Sci. Rep. 3, 2554. http://dx.doi.org/10.1038/srep02554.

AR2500 AcuityTM, n.d. Acuity AR2500 Specification [WWW Document]. URL www.acuitylaser.com (accessed 06.03.15.).

Government of Japan, 2011. Act on Special Measures Concerning the Handling of Radioactive Pollution. Government of Japan.

Hardie, S.M.L., McKinley, I.G., 2014. Fukushima remediation: status and overview of future plans. J. Environ. Radioact. 133, 75–85. http://dx.doi.org/10.1016/j.jenvrad.2013.08.002.

Jones, H.E., Cunningham, J.R., 1983. Physics of Radiology, fourth ed. Thomas Publishing, Springfield, Illinois, USA.

Kromek Group PLC, 2015. GR1 Spec Sheet; Revision 10 [WWW Document]. URL http://www.kromek.com/products_gr1spectrometer.asp (accessed 23.06.15.).

MacFarlane, J.W., Payton, O.D., Keatley, A.C., Scott, G.P.T., Pullin, H., Crane, R.A., Smilion, M., Popescu, I., Curlea, V., Scott, T.B., 2014. Lightweight aerial vehicles for monitoring, assessment and mapping of radiation anomalies. J. Environ. Radioact. 136, 127–130. http://dx.doi.org/10.1016/j.jenvrad.2014.05.008.

Martin, P.G., Payton, O.D., Fardoulis, J.S., Richards, D.A., Scott, T.B., 2015. The use of unmanned aerial systems for the mapping of legacy uranium mines. J. Environ. Radioact. 143, 135–140. http://dx.doi.org/10.1016/j.jenvrad.2015.02.004.

MEXT, 2011. Results of the Airborne Monitoring by the Ministry of Education, Culture, Sports, Science and Technology and the U.S. Department of Energy. 6th May 2011 [WWW Document]. URL. http://radioactivity.nsr.go.jp/en/contents/4000/3180/24/1304797_0506.pdf (accessed 02.03.15.).

Minty, B.R.S., 1997. Fundamental of airborne gamma-ray spectrometry. J. Aust. Geol. Geophys. 17, 39–50.

Minty, B.R.S., Luyendyk, A.P.J., Brodie, R.C., 1997. Calibration and data processing for airborne gamma-ray spectrometry. J. Aust. Geol. Geophys. 17, 51–62.

Mukai, H., Hatta, T., Kitazawa, H., Yamada, H., Yaita, T., Kogure, T., 2014. Speciation of radioactive soil particles in the Fukushima contaminated area by IP autoradiography and microanalyses. Environ. Sci. Technol. 48 (22), 13053–13059. http://dx.doi.org/10.1021/es502849e.

National Institute of Advanced Industrial Science and Technology, A., 2014. AIST Stories No.3. AIST Stories 21.

Sanada, Y., Kondo, A., Sugita, T., Nishizawa, Y., Youichi, Y., Kazutaka, I., Yasunori, S., Torii, T., 2014a. Radiation monitoring using an unmanned helicopter in the evacuation zone around the Fukushima Daiichi nuclear power plant. Explor. Geophys. 45 (1), 1–2.

Sanada, Y., Sugita, T., Nishizawa, Y., Kondo, A., Torii, T., 2014b. The aerial radiation monitoring in Japan after the Fukushima Daiichi nuclear power plant accident. Prog. Nucl. Sci. Technol. 4, 76–80. http://dx.doi.org/10.15669/pnst.4.76.

Sanada, Y., Torii, T., 2014. Aerial radiation monitoring around the Fukushima Daiichi nuclear power plant using an unmanned helicopter. J. Environ. Radioact. 139, 294–299. http://dx.doi.org/10.1016/j.jenvrad.2014.06.027.